Cell PRESS
Open ACCESS
Cell Reports
Resource

Spatial Representation of Odorant Valence in an Insect Brain

Markus Knaden,[1,*] Antonia Strutz,[1] Jawaid Ahsan,[1] Silke Sachse,[1] and Bill S. Hansson[1,*]
[1]Max Planck Institute for Chemical Ecology, Hans-Knöll Straße 8, 07745 Jena, Germany
*Correspondence: mknaden@ice.mpg.de (M.K.), hansson@ice.mpg.de (B.S.H.)
DOI 10.1016/j.celrep.2012.03.002

SUMMARY

Brains have to decide whether and how to respond to detected stimuli based on complex sensory input. The vinegar fly *Drosophila melanogaster* evaluates food sources based on olfactory cues. Here, we performed a behavioral screen using the vinegar fly and established the innate valence of 110 odorants. Our analysis of neuronal activation patterns evoked by attractive and aversive odorants suggests that even though the identity of odorants is coded by the set of activated receptors, the main representation of odorant valence is formed at the output level of the antennal lobe. The topographic clustering within the antennal lobe of valence-specific output neurons resembles a corresponding domain in the olfactory bulb of mice. The basal anatomical structure of the olfactory circuit between insects and vertebrates is known to be similar; our study suggests that the representation of odorant valence is as well.

INTRODUCTION

Animals make decisions by integrating a plethora of sensory inputs. In-depth analyses of the complete pathway from stimulus to decision are extremely rare because so many channels carry information to (or within) the brain. The well-characterized olfactory system of the vinegar fly *Drosophila melanogaster* does, however, offer unique possibilities for analyzing the decision-making process. Using simple cues, i.e., attractive and aversive monomolecular odorants, we aimed to characterize the pathway from ligand-receptor interactions to the formation of the first valence-specific brain activity patterns; these patterns should provide the substrate for decision making in the olfactory circuitry.

Drosophila melanogaster is today one of the three foremost models in olfactory research, paralleled only by the mouse and the nematode. Considerable insights into olfactory circuits have been achieved by combining neurogenetic tools with neurophysiology. One of the most important tasks for a fly is to locate and evaluate a substrate for feeding and oviposition. To perform this task, the fly depends on olfactory cues emitted by suitable substrates such as decaying fruit or unsuitable, e.g., toxic, substrates. Although such sources usually emit complex molecular blends, monomolecular odorants have also been described as attractive or aversive to flies (Dekker et al., 2006; Stensmyr et al., 2003).

Flies sense odorants using approximately 1,200 olfactory sensory neurons (OSNs) located in their antennae, and approximately 120 OSNs located in the maxillary palps (Shanbhag et al., 1999), the second olfactory organ. The OSNs represent the input to the first processing center, the antennal lobe (AL). Projecting onto spherical structures (so-called glomeruli), they target second-order neurons, the projection neurons (PNs) (Hildebrand and Shepherd, 1997). The PNs represent the output of the AL and convey olfactory information to higher brain centers such as the mushroom bodies and the lateral horn. Within the AL, OSNs as well as PNs are connected via local interneurons (LNs) that modulate OSN and PN activity (Wilson, 2008). OSNs are equipped with one out of 62 olfactory receptor types coded for in the *D. melanogaster* genome. OSNs expressing the same receptor gene(s) target the same glomerulus, and most PNs also send dendrites into a single glomerulus (Couto et al., 2005; Fishilevich and Vosshall, 2005; Vosshall et al., 2000). Each glomerulus can thus be considered a functional unit. The activation of some glomeruli are thought to be hard-wired to mediate behavioral responses; for example, glomerulus DM5 may mediate aversive behavior (Semmelhack and Wang, 2009). Since experiments to test this hypothesis were performed with only two olfactory stimuli, however, no general conclusions can be reached.

The most comprehensive study on receptor-ligand interactions so far tested a set of 24 *D. melanogaster* receptors against a total of 110 odorants (Hallem and Carlson, 2006). With this analysis as starting point, we screened the same set of odorants for their innate hedonic valence. Considering these values, we investigated the representation of odorant valence in the *D. melanogaster* brain. We correlated our behavioral data with the published single-sensillum recording (SSR) data (Hallem and Carlson, 2006), and performed functional imaging experiments using the six most attractive and six most aversive odorants at the level of input (OSNs) and output neurons (PNs) of the AL. Although we found only weak valence-specific activity at the OSN level, attractive and aversive odorants could be well discriminated based on the observed activity patterns at the level of PNs. We identified six glomeruli in which an output response was evoked almost exclusively by aversive odorants and three glomeruli in which an output response was triggered mainly by attractive odorants. By characterizing the spatial coding patterns that are elicited by a set of odorants with known valence from the periphery to the brain, we were able to relate the first level of hedonic valence representation to the output level of the AL.

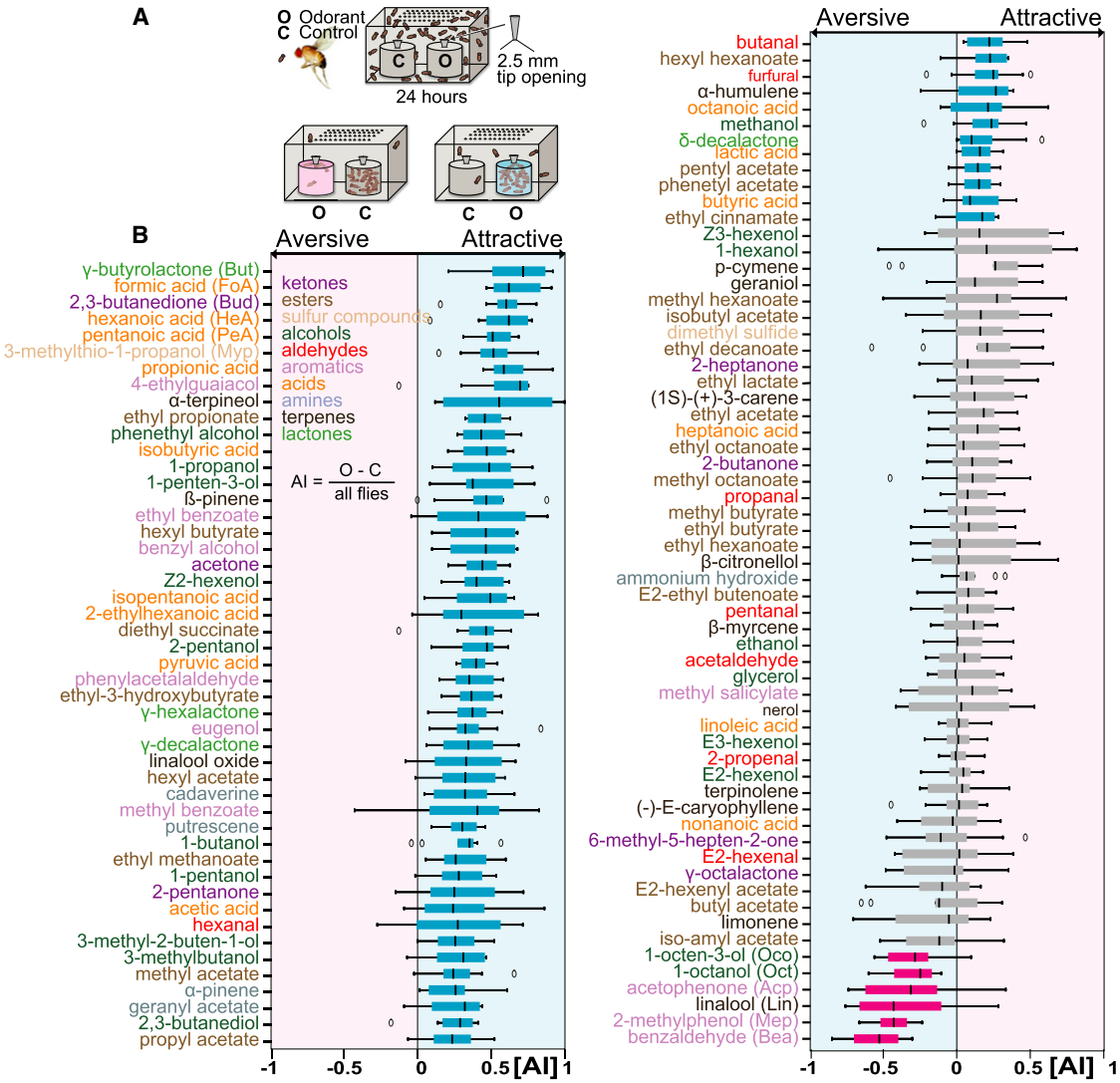

Figure 1. Hedonic Valence of Odorants

(A) Trap assay. Fifty flies (black circles) were free to choose between two traps with one trap containing the odorant plus solvent and the other containing the solvent only. The only access for the odorant molecules into the bioassay chamber was through the 2.5 mm pipette tip opening through which flies entered the traps. Flies in both traps were counted after 24 hr. For details of analysis, see Experimental Procedures. For an analysis of the concentration changes within the assay during 24 hr, see Figure S1.

(B) Attraction indices of 110 odorants. Odorants are sorted according to attractiveness. Turquoise, attractive odorants with attraction index (AI) being significantly ($p < 0.05$, Wilcoxon rank sum test) larger than 0; gray, neutral odorants with AI not differing from 0; magenta, aversive odorants with AI significantly ($p < 0.05$) smaller than 0. Box plots give the median (black bold line), quartiles (box), 95% confidence intervals (whiskers), and outliers (gray circles) of the ten replicated trap-assay tests with each odorant. Functional groups of the odorants are color-coded.

RESULTS

Hedonic Valence of Odorants

Using a trap assay modified from previously described assays (Larsson et al., 2004; Park et al., 2002) (Figure 1A), we screened 110 odorants for their valence. For an analysis of the concentration changes within the assay during 24 hr, see Figure S1. We classified 60 as attractive, 44 as neutral, and only 6 odorants as aversive (Figure 1B). With a median attraction index (AI) of 0.72 (Figure 1B), γ-butyrolactone was the most attractive compound, whereas benzaldehyde was the most aversive one (median AI: −0.53). We could not find any correlation between classical chemical structure and odorant valence, since both highly attractive and neutral compounds were found in each chemical class (color-coded in Figure 1B). Moreover, the six aversive odorants belonged to three different chemical classes (alcohols, aromatics, and terpenes), which also included highly attractive substances.

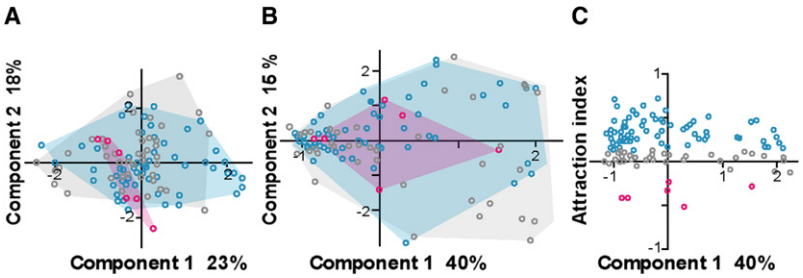

Figure 2. Analysis of Physicochemical and Physiological Properties of Attractive and Aversive Odorants

(A and B) Principal component analyses (PCA) of attractive (turquoise) and aversive (magenta) odorants based (A) on their physicochemical properties (i.e., a set of 32 physicochemical descriptors; Haddad et al., 2008) and (B) on published single sensillum recordings (Hallem and Carlson, 2006).

(C) Correlation between first principal component (based on single-sensillum recording data) and attraction indices (AI) of the odorants.

Correlation of Hedonic Valence and Physicochemical Properties

Haddad et al. (2008) suggested that the olfactory percept of a substance relies not simply on its chemical class but on numerous additional molecular descriptors. We asked if these physicochemical properties account for the innate valence. However, using a principal component analysis (PCA, Figure 2A), we did not find any coherent clustering of attractive and aversive odorants. Neither did we find any correlation between the Euclidean distance of odorant pairs based on their physicochemical properties and the distance between the odorants' hedonic valence (Figure S2A; Table S1).

Peripheral Representation of Valence

Hallem and Carlson (2006) provided information regarding which out of 24 *D. melanogaster* OSNs investigated was activated by the 110 odorants tested. We wondered whether we could predict the valence of these odorants on the basis of the activated olfactory receptor repertoire (for a chart of all used SSR data from Hallem and Carlson, 2006; see Table S1). Again, a PCA (Figure 2B) and a calculation of the Euclidean distance between odorants (Figure S2B) performed with the published raw data (Hallem and Carlson, 2006) was inconclusive in predicting the hedonic valence of the odorants. Neither attractive nor aversive odorants clustered in the PCA (Figure 2B), and the first principal component of the same data set did not correlate with the odorant attraction indices (Figure 2C). A correlation of the first principal component with odorant valence was found in an earlier study by Haddad et al. (2010), analyzing *D. melanogaster* neuronal responses and preferences for seven odorants. Our results, however, obtained with 110 odorants, showed no representation of odorant valence at the level of the antenna.

Representation of Valence in the AL

We next identified the AL glomeruli that became activated by the six most attractive and the six most aversive odorants. To investigate the input as well as the output of the AL, we used the standard GAL4-UAS system (Brand and Perrimon, 1993) to drive expression of the genetically encoded calcium sensor G-CaMP and thus labeled either OSNs or PNs (Figure 3).

All stimuli produced multiglomerular activation patterns in the AL (for a topographic visualization of activity patterns, see Figure S3; for numerical information on glomerular activations, see Table S2; for identification of activated glomeruli, see Stökl et al., 2010; for a validation of glomerular identification by use of a two-photon imaging setup, see Supplemental Information). At the OSN level, individual glomeruli were similarly activated by attractive and aversive odorants; i.e., attractive and aversive odorants were not separated in a PCA based on activation patterns (Figure 4A) and the hedonic distances of odorant pairs were not correlated with their Euclidean distances based on OSN responses (Figure S2C). As expected, the activation of OSNs at the glomerular level strongly correlated (Figures S2G and S2H) with the corresponding published SSR data (Hallem and Carlson, 2006), confirming a correct glomeruli identification.

At the PN level, however, the subsets of glomeruli activated by attractive odorants differed significantly from those activated by aversive odorants (Table S2). Euclidean distances based on hedonic distances of odorant pairs significantly correlated with Euclidean distances based on PN activation patterns (Mantel test, $p < 0.01$; Figures S2D and S2F). The latter accounted for 5%–18% of the variability of the distances of hedonic valences, i.e., significantly more than calculated for the impact of physicochemical properties (0.3%), single sensillum responses (0.4%), and OSN responses in the AL (0.07%–0.2%) (Figures S2A–S2C and S2E). PNs innervating glomeruli DL5, D, and DL1 were activated almost exclusively by aversive odorants, whereas DM4, DM5, and DM2 became mainly activated by attractive odorants (Figure 4B, right panel), resulting in a separation of attractive and aversive odorants in an activation pattern-based PCA (Figure 4B).

To investigate whether the observed result depends on the concentration of the stimulus, we repeated the functional imaging experiments with stimulus concentrations increased by two orders of magnitude (10^{-2}; Figure S3; Table S2). Again, no clear valence-specific pattern at the OSN level could be detected (Figure 4C). Only three glomeruli (DA4, DC2, and DC3) responded significantly discriminatively to aversive and attractive odorants resulting in a weak separation of attractive and aversive odorants (Figure 4C). However, probably due to the strong but nondiscriminative response of several other glomeruli, this separation was along principal component 2 that contributed less to the variance than principal component 1. Therefore, the split of attractive and aversive odorants at the level of OSNs was not significant ($p = 0.77$).

On the contrary, PN patterns were clearly valence dependent (Figure 4D). At the higher stimulus concentration, no glomerulus was exclusively activated by attractive odorants. However, six glomeruli (D, DA4, DL1, DL4, DL5, and DC3, see Figure 4D) responded strongly and mainly to aversive odorants, which substantiates their function as "aversive-specific" glomeruli, at

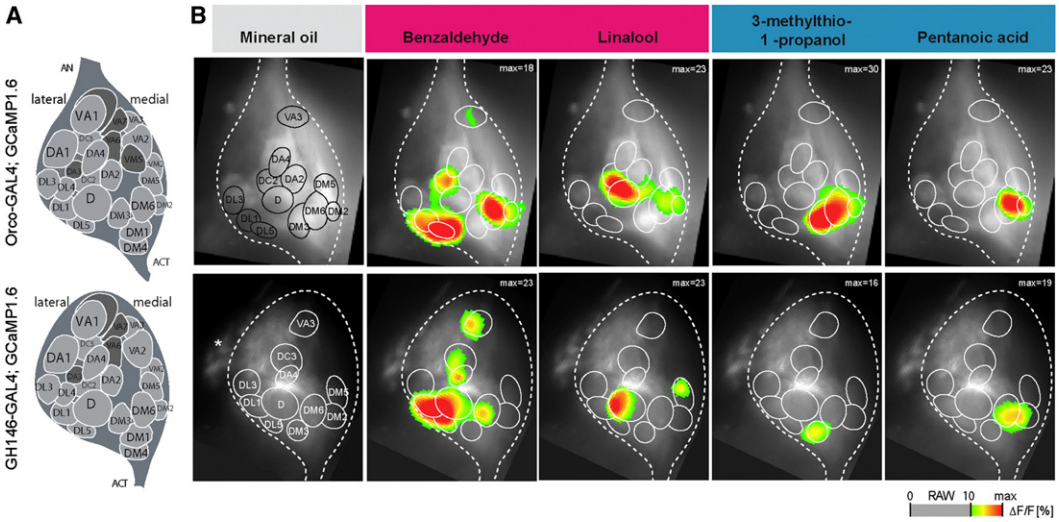

Figure 3. Identification of Glomeruli Activated by Attractive and Aversive Odorants Using Functional Calcium Imaging

(A) Schematized atlas of the AL representing glomeruli that have been functionally characterized. Flies expressing the genetically encoded calcium reporter G-CaMP allowed us to visualize odorant-evoked activities at the level of OSNs (top panels) and PNs (bottom panels) using the Orco-GAL4 and GH146-GAL4 line, respectively. Both lines label an overlapping set of glomeruli with the exception of glomerulus VM5, which is not labeled by the GH146 driver line. Glomeruli that were not significantly activated by any of the odorants are filled in dark gray. AN, antennal nerve; ACT, antennocerebral tract.

(B) Representative false color-coded images showing the AL after stimulation with mineral oil as a control or with aversive (magenta) and attractive (turquoise) odorants. All images are individually scaled to the strongest activated glomeruli of the entire AL (data shown only for the left AL). Values below the ΔF/F threshold of 10% are omitted to illustrate the specificity of the signals, as well as the glomerular arrangement as visualized by the intrinsic fluorescence. Images represent ΔF/F [%] superimposed onto the raw fluorescence images according to the scale below. White asterisk marks the PN soma cluster.

For observed activation patterns see Figure S3 and Table S2.

least when they become activated in a combinatorial pattern. Hence, the finding that there is already a representation of odorant valence at the output of the AL holds true over a concentration range of at least two orders of magnitude.

Interestingly, those PNs that were significantly more activated by aversive odorants innervated glomeruli clustered topographically in the lateral part of the AL, whereas the attractant-specific PNs innervated glomeruli located at the medial part (inset in right panels of Figures 4B and 4D, median distance between glomeruli activated by odorants of similar hedonic valence, 23 μm; median distance between glomeruli activated by odorants of different hedonic valence, 43 μm; Mantel test, $p < 0.001$).

DISCUSSION

Drosophila melanogaster responds behaviorally to numerous odorants. So far, only one study has dissected the flies' responses to a large set of odorants. This study, however, focused on response latencies and olfactory sensitivities but not on the hedonic valence of these odorants (Keller and Vosshall, 2007). Here, we present the most comprehensive screen for odorant valence performed so far in *D. melanogaster*. Our results allowed us to assign the first clear representation of hedonic valence in the *D. melanogaster* olfactory circuitry to the AL output level.

An odorant's identity has been shown to be determined by numerous physicochemical properties, which, in turn, are decisive for the set of OSNs (and thereby receptors) activated by this odorant (Haddad et al., 2008). Furthermore, in a meta-analysis of 12 data sets, including separate studies in seven species, the results of seven odorants tested in *D. melanogaster* suggested that the specific set of receptors activated by an odorant accounts for its hedonic valence (Haddad et al., 2010). In contrast, neither the physicochemical properties of the 110 odorants used here (out of which four were included in the study with seven compounds) (Figure 2A), nor the activated receptor repertoire (Figure 2B, in which we reanalyzed the SSR data obtained with the same 110 odorants by Hallem and Carlson, 2006) predicted the valence of the tested odorants. However, as our set of 110 odorants included only four of the seven odorants analyzed by Haddad et al. (2010), it is difficult to draw any conclusions regarding the background to the contradicting results. In humans, Khan et al. (2007) found a strong correlation between physicochemical properties and hedonic valence of odorants. We can only speculate, that this difference between flies and humans is caused by different coding strategies for innate hedonic valence, as suggested by the findings of Keller and Vosshall (2007), showing that olfactory similarity judgment clearly differs between flies and humans. Functional imaging of calcium activity in OSNs enabled us to analyze activity of 20 OSN types targeting the top layer of the glomeruli (i.e., 60% of all OSNs labeled by Orco-GAL4), 8 of which were not included in the SSR study (Hallem and Carlson, 2006). Processing of olfactory information already starts at the level of OSNs via presynaptic inhibition (Olsen and Wilson, 2008; Root et al., 2008). Hence, the odorant-evoked glomerular responses monitored by functional imaging of OSNs at the level of the AL do not necessarily mirror the results gained at the level of the

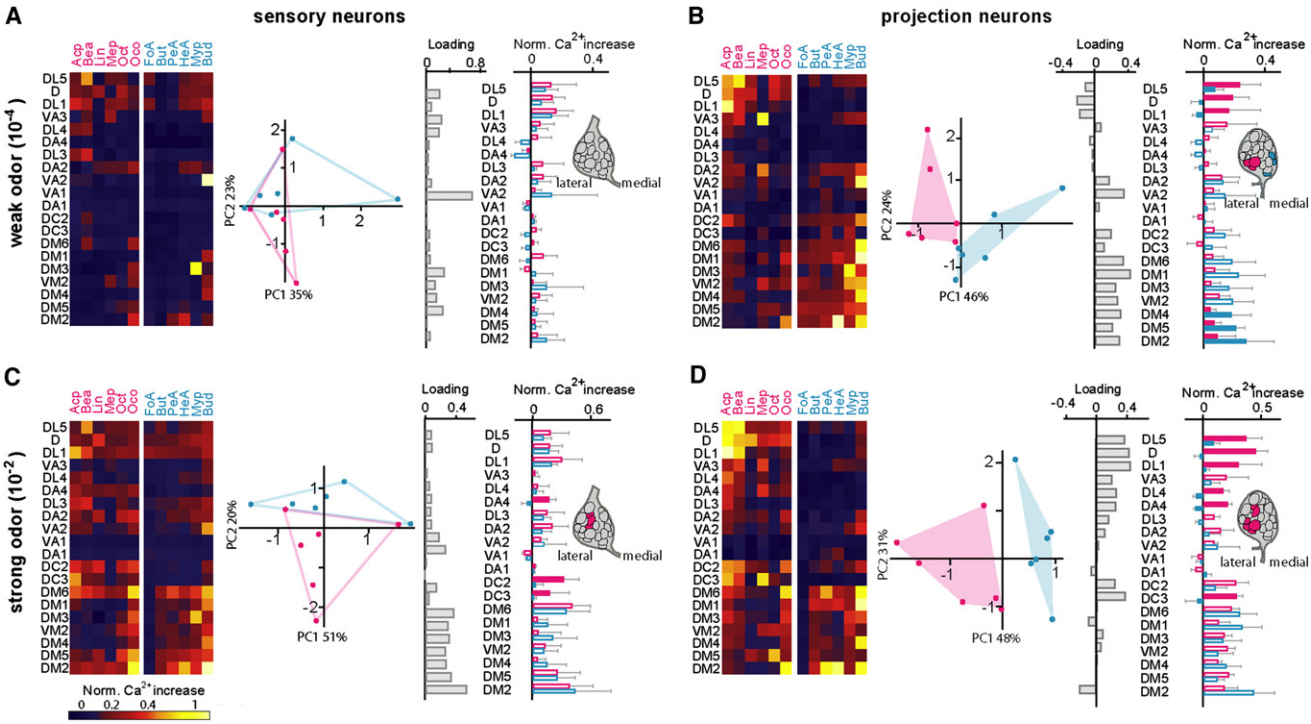

Figure 4. Representation of Odorants within the Antennal Lobe

(A and B) OSNs (A) and PNs (B) at weak stimulus concentrations.

(C and D) OSNs (C) and PNs (D) at strong stimulus concentrations.

Left panels, principal component analyses based on the activation patterns elicited by the 12 odorants tested (see Table S2). Representation of attractive odorants differed from aversive ones at the PN level (ANOSIM, Bray-Curtis, weak concentration, $p < 0.005$, strong concentration, $p < 0.002$) but not at the level of OSNs (weak concentration, $p = 0.79$, strong concentration, $p = 0.77$). Centre panels, bar graphs depicting the weight by which the activation of each glomerulus affects the first principal component. Right panels, activation of individual glomeruli by attractive (turquoise) and aversive (magenta) odorants; bar plots depict average response and standard deviation of six stimulations with attractive and with aversive odorants. Solid bars depict glomeruli that differ significantly in their response to attractive and aversive odorants ($p < 0.05$, Mann-Whitney test). Inset depicts the spatial distribution of glomeruli that discriminatively responded to attractive or aversive odorants.

antennae entirely. Nevertheless, the glomerular activation patterns we observed at the AL input level resembled those of the corresponding receptors on the antennae (Figures S2G and S2H). Only three glomeruli (DA4, DC2, and DC3, Figure 4C) did respond significantly and discriminatively to attractive as well as aversive odorants. Since several other glomeruli exhibited stronger responses but did not respond discriminatively, attractive and aversive odorants were not significantly separated based on the OSN activity pattern (Figures 4A and 4C).

The scenario changed when we analyzed activity patterns at the next processing level, the PNs. Here, we identified a large set of strongly activated glomeruli that responded discriminatively to attractive and aversive odorants. Glomeruli DM4, DM5, and DM2 were significantly stronger activated by attractive components, whereas D, DA4, DC3, DL1, DL4, and DL5 responded almost exclusively to aversive odorants (Figures 4B and 4D, right panels). Therefore, based on the PN activity patterns, attractive and aversive odorants could be clearly separated (Figures 4B and 4D). Interestingly DA4 and DC3 were identified as "aversive specific" both at the input (Figure 4C) and output levels (Figure 4D).

In another study that combined functional imaging and behavioral experiments, Semmelhack and Wang (2009) determined the role of several glomeruli in mediating responses to different concentrations of cider vinegar. The authors identified DM1 and VA2 as mediators of attraction to vinegar, whereas DM5 was assigned as responsible for aversive behavior at high stimulus concentrations. In light of these results, the authors suggested DM5 to be hard-wired for generating innate aversive behavior. We instead observed the DM5 to be strongly activated by various attractive odorants at least at the PN level (Figure 4B, right panel). What could have caused these inconsistent results? An interesting outcome of the vinegar study, which used an olfactometer and tested for immediate responses within 50–250 s, was that the valence of a blend was highly affected by its concentration. The valence of vinegar changed when the concentration was increased by less than one order of magnitude. In the trap assay, in which flies were tested in still air for 24 hr, a blend has earlier been shown to be attractive over five orders of magnitude (Stökl et al., 2010) (for the time course of concentration changes within the trap assay, see Figure S1). It could thus be speculated that the glomeruli identified by

Semmelhack and Wang as aversive specific (Semmelhack and Wang, 2009) might generate a concentration-dependent immediate response to odorants, whereas the valence-specific PN patterns described by us are less concentration dependent and seem to be valid for flies that can decide unhurriedly whether or not to approach an odorant. Interestingly, Semmelhack and Wang (2009) found the same glomerulus DM5 involved in mediating aversion to both the vinegar bouquet as well as an individual odorant (ethyl butyrate) that is not present in vinegar. As flies usually perceive blends rather than individual odorants, it is of interest whether the coding and rating of blends can be predicted by the coding and rating of the blends' individual components. Our screen of 110 odorants provides a vantage point for such an investigation.

In *D. melanogaster* larvae, the valence of odorants could be predicted based on the activation patterns of a set of specific receptors (Kreher et al., 2008), i.e., at the periphery of the olfactory circuitry. However, the larval olfactory system shows striking differences to the adult system, as it is for example greatly reduced in every way, and thus cannot be expected to perform in a similar fashion as the adult one. The systems differ both regarding the number of OSNs and the kind of olfactory receptors expressed in these. Larvae have 21 OSNs expressing 25 receptors (Fishilevich et al., 2005), whereas adults have approximately 1,200 OSNs expressing 62 receptors with an overlap between adults and larvae of only 11 receptors (Shanbhag et al., 1999). It would have been interesting to analyze, whether OSNs that are expressed both in larvae and adults respond differentially to the same set of odors. However, of the 11 larval OSNs investigated by Kreher et al. (2008) only two are expressed in adult flies and were included in our study. Due to this small overlap, no conclusions can be drawn regarding the odorant specificity of OSNs that are expressed both in larvae and adult flies. The difference at the peripheral olfactory sensory system very likely reflects different demands on the olfactory performance of larvae and of adults. Larvae hatch on food and usually migrate within a range of only a few centimeters, i.e., nutritional decisions are made by the adult fly during oviposition. Before ovipositing, the adult fly needs to detect and evaluate food sources at a distance and often against an olfactory background. This behavior probably requires increasing numbers of OSNs and receptors in adult flies. This increased capacity might occur due to the observed drift of the first representation of valence from the sensory periphery to the brain, as the information processing within the AL can help flies to predict the meaning of an odorant. Interestingly, both larvae and adult flies were repelled by methylphenol and benzaldehyde. The former is a typical mammalian odorant that is used by blood-feeding insects to locate hosts but seems to be avoided by plant-feeding insects (Hill et al., 2010). The latter is a by-product of the production of hydrocyanic acid in seeds, and serves as a defense against herbivores (Peterson et al., 1987). Hence, by avoiding benzaldehyde, flies and larvae may keep a safe distance from poisonous seeds. It should be mentioned that benzaldehyde has been shown to be a multimodal stimulus affecting nociceptive as well as olfactory pathways (Keene et al., 2004). However, as it produces aversive-specific responses at the PN level of the AL, the olfactory pathway is involved in dictating the hedonic valence of this stimulus.

There is an ongoing debate about how much olfactory information is processed within the AL. Some studies found identical activity patterns in OSNs and corresponding PNs (Semmelhack and Wang, 2009; Wang et al., 2003), while others (Bhandawat et al., 2007; Root et al., 2008; Wilson et al., 2004) suggested different odorant representations at the two levels. The existence of a representation of hedonic valence at the PN level but not at the level of OSNs supports the argument that a considerable amount of information is being processed, most likely by the complex network formed by local interneurons (Chou et al., 2010; Seki et al., 2010).

Ants classify other ants as nestmates or nonnestmates by comparing their cuticular hydrocarbon profile with a learned template (Leonhardt et al., 2007). Agreement of profile and template leads to acceptance, while disagreement leads to aggression. Contrary to our findings in flies, no neuronal correlate of this classification was found in the ants' antennal lobe. Nestmate and nonnestmate odors elicited similar activity patterns in calcium imaging experiments (Brandstaetter et al., 2011). However, while flies should have an innate idea whether an odor means food or not, nestmate recognition in ants depends on an ongoing learning process, i.e., the reformation of their internal template (Leonhardt et al., 2007). Therefore, it is likely that nestmate classification rather takes place in higher brain centers like the mushroom bodies that have been shown to be involved in Hymenopteran olfactory learning (Hourcade et al., 2010).

Interestingly, glomeruli that we found to be activated mainly by aversive odorants formed a cluster at the lateral part of the AL (Figures 4B and 4D), whereas those that became more activated by attractive odorants clustered at the medial part (Figure 4B). Accordingly, we propose that two functional areas, located at the output level of the AL and composed of glomerular clusters, embody the first representation of hedonic valence of an odorant. This finding is in accordance with results from mice and humans, where the dorsal domain of the olfactory bulb seems to be responsible for innate responses to aversive odorants (Kobayakawa et al., 2007; Rolls et al., 2003). Further studies should examine how the representation of valence in flies is transferred to higher brain centers and ask whether the representation is affected by learning. The identification of a large set of innately attractive and aversive odorants is also an excellent springboard for further studies on odorant-guided behavior in flies.

Our study is based on the establishment of the hedonic valence of 110 odorants, with known physicochemical properties (Haddad et al., 2008) and peripheral neurophysiological impact (Hallem and Carlson, 2006). These values in combination with the establishment of input and output activation patterns in the AL made it possible to conduct the first in-depth analysis of the pathway from ligand-receptor interactions to the formation of the first valence-specific patterns; such a pathway constitutes the basis for decision making in the insect brain.

EXPERIMENTAL PROCEDURES

Behavior

To screen the attractiveness of a total of 110 odorants, we modified a trap assay that has been used to determine differences in odorant-guided behavior between different genotypes or species of *Drosophila* (Dekker et al., 2006;

Larsson et al., 2004; Ruebenbauer et al., 2008). Test chambers (transparent yoghurt cups (500 ml) with 50 ventilation holes in the lid) contained a treatment and a control trap made from small transparent plastic vials (30 ml) with a cut micropipette tip (tip diameter 2 mm) inserted into a hole of the vial. The treatment trap contained 2 μl of the test odorant diluted in 200 μl of water (plus 0.2 μl Triton X-100 [http://www.sigmaaldrich.com]) as detergent applied on a piece of filter paper, while the control trap contained only 200 μl of water plus 0.2 μl Triton X-100. Fifty flies (males and females, ratio about 1:1, 4–5 days old, starved for 24 hr before the experiment) were placed in each test box (Figure 1). Experiments were always started at the same time of day and carried out in a climate chamber (25°C, 70% humidity, 12-hr-light:12-hr-dark cycle). The number of flies in and outside the traps was counted after 24 hr. Valence of the tested odorants was quantified with an AI, calculated as: AI = (O-C)/(50), where O is the number of flies in the odorant trap, C the number of flies in the control trap, and 50 the sum of all flies tested. The resulting index ranges from −1 (complete avoidance) to 1 (complete attraction). A value of zero characterizes a neutral or nondetected odorant. Deviation of the AI from zero and differences of the AI between groups were tested with the Wilcoxon rank sum test.

For an analysis of the concentration changes within the assay during 24 hr, see Figure S1.

Functional Imaging

Fly Preparation

In vivo preparation of flies (5 to 8 days old animals) and functional imaging of odor-evoked calcium responses in the AL were essentially as described (Strutz et al., 2012; Stökl et al., 2010). Briefly, flies were anesthetized on ice for 15 min, fixed with the neck onto a Plexiglas stage using a copper plate (Athene Grids, http://www.tedpella.com). The head was glued on the stage with colophony resin (Royal Oak Rosinio, http://www.bandbuddy.com) and the antennae pulled forward with a fine metal wire (http://www.hpreid.com). Polyethylene foil was attached on the head and sealed to the cuticle with two-component silicone (http://www.wpiinc.com). A small window was cut through the foil and cuticle. Immediately after opening the head capsule, the brain was bathed with Ringer solution (130 mM NaCl, 5 mM KCl, 2 mM $MgCl(x\ 6H_2O)$, 2 mM $CaCl_2(x\ 2H_2O)$, 36 mM Saccharose, 5 mM HEPES, [pH 7.3]). Removal of trachea and glands allowed optical access to the ALs.

Odorant Stimulation

Odorants were diluted (10^{-1} or 10^{-3}) in mineral oil (http://www.sigmaaldrich.com). 6 μl of the diluted odorants was pipetted onto a small piece of filter paper (~1 cm^2, http://www.whatman.com), placed inside a glass Pasteur pipette. For odorant application, a stimulus controller (Stimulus Controller CS-55, http://www.syntech.nl) was used, which produced a continuous airstream, whose flow of 1 l min^{-1} was monitored by a flowmeter (http://www.coleparmer.com). A glass tube guided the airflow to the fly's antennae. Within the constant air stream, the applied odorant stimuli were additionally diluted by 1:10.

Functional Imaging

Imaging experiments were performed using a TillPhotonics imaging setup (TILL imago, http://www.till-photonics.com) equipped with a CCD-camera (PCO imaging, http://www.pco.de) mounted on a fluorescence microscope (BX51WI, http://www.olympus.com) with a 20x water immersion objective (NA 0.95, XLUM Plan FI, http://www.olympus.com). A monochromator (Polychrome V, TillPhotonics) produced a 475 nm excitation wavelength, which passed a SP500 filter, a dichromatic mirror (DCLP490) and finally a LP515 filter before reaching the animal. Binning on the CCD-camera chip produced a resolution of 1.2 μm $pixel^{-1}$. Each recording lasted 10 s with an acquisition rate of 4 Hz. Odorants were applied during frames 6–14 (i.e., after 1.5 s, lasting for 2 s). Experiments with single flies lasted up to 1 hr, with intervals between stimuli of about 1 min. The two GAL4 driver lines, Orco and GH146 label 33 and 31 glomeruli, respectively (unpublished data). Using functional imaging we were able to characterize the response profile of glomeruli in the top layer of the antennal lobe. This group comprises 20 glomeruli and covers about 60% of all glomeruli labeled by the Orco-GAL4 as well as the GH146-GAL4 driver lines. All visible glomeruli during our imaging experiments were thus labeled by both lines, with the exception of glomerulus VM5, which is labeled by Orco but not by GH146. This glomerulus was therefore excluded from the analysis (see Figure 3).

Image Analysis

Data were analyzed with custom-written IDL software (ITT Visual Information Solutions, http://www.ittvis.com) provided by Mathias Ditzen and Giovanni Galizia, Germany. All recordings were manually corrected for movement. To achieve a comparable standard for the calculation of the relative fluorescence changes (ΔF/F), the fluorescence background was subtracted from the averaged values of frames 0 to 6 in each measurement, so that basal fluorescence was normalized to zero. The false color-coded fluorescence changes in the raw-data images have been calculated by subtracting frame 7 from frame 12. To calculate the response of a specific glomerulus to each odorant, a coordinate (10×10 μm) was placed in the center of an identified glomerulus and the fluorescent changes were plotted as a function of time. Subsequently, the mean value of frames 10 to 17 (response maximum during odorant stimulation) of a specific glomerulus and odorant was calculated and averaged over all animals. Glomerular identification was performed as described in detail in Stökl et al. (2010) (see also Supplemental Information). Neither of the used fly strains (see below) allowed us to visualize the activity of glomeruli innervated by ionotropic receptors (IRs), which may play an additional role in coding odorant valence. However, our approach allowed us to selectively visualize the odorant-evoked glomerular activity pattern of the input and output neurons of 20 glomeruli of the AL (Table S2). The activated glomeruli were identified using the well-defined OSN glomerular connectivity map of the fly AL (Couto et al., 2005; Fishilevich and Vosshall, 2005). Additionally, we screened a set of odorants with defined activation patterns to facilitate glomerular identification (e.g., DM5, ethyl-3-hydroxybutyrate; DM2, ethyl hexanoate; DM6, pentylacetate).

Fly Strains

For the calcium imaging experiments, we used the standard GAL4-UAS system (Brand and Perrimon, 1993) to genetically express the calcium-sensitive protein G-CaMP 1.6 (Ohkura et al., 2005) in either the majority of OSNs or PNs using the Orco-GAL4 or GH146-GAL4 driver line, respectively.

SUPPLEMENTAL INFORMATION

Supplemental Information includes Extended Experimental Procedures, three figures, and two tables and can be found with this article online at doi:10.1016/j.celrep.2012.03.002.

LICENSING INFORMATION

ACKNOWLEDGMENTS

This study was supported by fundings from the Max Planck Society to BSH and from the Bundesministerium für Bildung und Forschung (BMBF) to S.S. We would like to thank Mrs. E. Wheeler for editorial assistance and Dr. M.C. Stensmyr and Ms. Tali Weiss for comments on the manuscript.

Received: November 4, 2011
Revised: March 5, 2012
Accepted: March 8, 2012
Published online: April 12, 2012

REFERENCES

Bhandawat, V., Olsen, S.R., Gouwens, N.W., Schlief, M.L., and Wilson, R.I. (2007). Sensory processing in the Drosophila antennal lobe increases reliability and separability of ensemble odor representations. Nat. Neurosci. *10*, 1474–1482.

Brand, A.H., and Perrimon, N. (1993). Targeted gene expression as a means of altering cell fates and generating dominant phenotypes. Development *118*, 401–415.

Brandstaetter, A.S., Rössler, W., and Kleineidam, C.J. (2011). Friends and foes from an ant brain's point of view—neuronal correlates of colony odors in a social insect. PLoS ONE *6*, e21383.

Chou, Y.H., Spletter, M.L., Yaksi, E., Leong, J.C.S., Wilson, R.I., and Luo, L.Q. (2010). Diversity and wiring variability of olfactory local interneurons in the Drosophila antennal lobe. Nat. Neurosci. *13*, 439–449.

Couto, A., Alenius, M., and Dickson, B.J. (2005). Molecular, anatomical, and functional organization of the Drosophila olfactory system. Curr. Biol. *15*, 1535–1547.

Dekker, T., Ibba, I., Siju, K.P., Stensmyr, M.C., and Hansson, B.S. (2006). Olfactory shifts parallel superspecialism for toxic fruit in Drosophila melanogaster sibling, D. sechellia. Curr. Biol. *16*, 101–109.

Fishilevich, E., and Vosshall, L.B. (2005). Genetic and functional subdivision of the Drosophila antennal lobe. Curr. Biol. *15*, 1548–1553.

Fishilevich, E., Domingos, A.I., Asahina, K., Naef, F., Vosshall, L.B., and Louis, M. (2005). Chemotaxis behavior mediated by single larval olfactory neurons in Drosophila. Curr. Biol. *15*, 2086–2096.

Haddad, R., Khan, R., Takahashi, Y.K., Mori, K., Harel, D., and Sobel, N. (2008). A metric for odorant comparison. Nat. Methods *5*, 425–429.

Haddad, R., Weiss, T., Khan, R., Nadler, B., Mandairon, N., Bensafi, M., Schneidman, E., and Sobel, N. (2010). Global features of neural activity in the olfactory system form a parallel code that predicts olfactory behavior and perception. J. Neurosci. *30*, 9017–9026.

Hallem, E.A., and Carlson, J.R. (2006). Coding of odors by a receptor repertoire. Cell *125*, 143–160.

Hildebrand, J.G., and Shepherd, G.M. (1997). Mechanisms of olfactory discrimination: converging evidence for common principles across phyla. Annu. Rev. Neurosci. *20*, 595–631.

Hill, S.R., Zaspel, J., Weller, S., Hansson, B.S., and Ignell, R. (2010). To be or not to be… a vampire: a matter of sensillum numbers in Calyptra thalictri? Arthropod Struct. Dev. *39*, 322–333.

Hourcade, B., Muenz, T.S., Sandoz, J.C., Rössler, W., and Devaud, J.M. (2010). Long-term memory leads to synaptic reorganization in the mushroom bodies: a memory trace in the insect brain? J. Neurosci. *30*, 6461–6465.

Keene, A.C., Stratmann, M., Keller, A., Perrat, P.N., Vosshall, L.B., and Waddell, S. (2004). Diverse odor-conditioned memories require uniquely timed dorsal paired medial neuron output. Neuron *44*, 521–533.

Keller, A., and Vosshall, L.B. (2007). Influence of odorant receptor repertoire on odor perception in humans and fruit flies. Proc. Natl. Acad. Sci. USA *104*, 5614–5619.

Khan, R.M., Luk, C.H., Flinker, A., Aggarwal, A., Lapid, H., Haddad, R., and Sobel, N. (2007). Predicting odor pleasantness from odorant structure: pleasantness as a reflection of the physical world. J. Neurosci. *27*, 10015–10023.

Kobayakawa, K., Kobayakawa, R., Matsumoto, H., Oka, Y., Imai, T., Ikawa, M., Okabe, M., Ikeda, T., Itohara, S., Kikusui, T., et al. (2007). Innate versus learned odour processing in the mouse olfactory bulb. Nature *450*, 503–508.

Kreher, S.A., Mathew, D., Kim, J., and Carlson, J.R. (2008). Translation of sensory input into behavioral output via an olfactory system. Neuron *59*, 110–124.

Larsson, M.C., Domingos, A.I., Jones, W.D., Chiappe, M.E., Amrein, H., and Vosshall, L.B. (2004). Or83b encodes a broadly expressed odorant receptor essential for Drosophila olfaction. Neuron *43*, 703–714.

Leonhardt, S.D., Brandstaetter, A.S., and Kleineidam, C.J. (2007). Reformation process of the neuronal template for nestmate-recognition cues in the carpenter ant Camponotus floridanus. J. Comp. Physiol. A Neuroethol. Sens. Neural Behav. Physiol. *193*, 993–1000.

Ohkura, M., Matsuzaki, M., Kasai, H., Imoto, K., and Nakai, J. (2005). Genetically encoded bright Ca2+ probe applicable for dynamic Ca2+ imaging of dendritic spines. Anal. Chem. *77*, 5861–5869.

Olsen, S.R., and Wilson, R.I. (2008). Lateral presynaptic inhibition mediates gain control in an olfactory circuit. Nature *452*, 956–960.

Park, S.K., Shanbhag, S.R., Dubin, A.E., de Bruyne, M., Wang, Q., Yu, P., Shimoni, N., D'Mello, S., Carlson, J.R., Harris, G.L., et al. (2002). Inactivation of olfactory sensilla of a single morphological type differentially affects the response of Drosophila to odors. J. Neurobiol. *51*, 248–260.

Peterson, S.C., Johnson, N.D., and Leguyader, J.L. (1987). Defensive regurgitation of allelochemicals derived from host cyanogenesis by Eastern tent caterpillars. Ecology *68*, 1268–1272.

Rolls, E.T., Kringelbach, M.L., and de Araujo, I.E.T. (2003). Different representations of pleasant and unpleasant odours in the human brain. Eur. J. Neurosci. *18*, 695–703.

Root, C.M., Masuyama, K., Green, D.S., Enell, L.E., Nässel, D.R., Lee, C.H., and Wang, J.W. (2008). A presynaptic gain control mechanism fine-tunes olfactory behavior. Neuron *59*, 311–321.

Ruebenbauer, A., Schlyter, F., Hansson, B.S., Löfstedt, C., and Larsson, M.C. (2008). Genetic variability and robustness of host odor preference in Drosophila melanogaster. Curr. Biol. *18*, 1438–1443.

Seki, Y., Rybak, J., Wicher, D., Sachse, S., and Hansson, B.S. (2010). Physiological and morphological characterization of local interneurons in the Drosophila antennal lobe. J. Neurophysiol. *104*, 1007–1019.

Semmelhack, J.L., and Wang, J.W. (2009). Select Drosophila glomeruli mediate innate olfactory attraction and aversion. Nature *459*, 218–223.

Shanbhag, S.R., Muller, B., and Steinbrecht, R.A. (1999). Atlas of olfactory organs of Drosophila melanogaster - 1. Types, external organization, innervation and distribution of olfactory sensilla. Int. J. Insect Morphol. Embryol. *28*, 377–397.

Silbering, A.F., Rytz, R., Grosjean, Y., Abuin, L., Ramdya, P., Jefferis, G.S.X.E., and Benton, R. (2011). Complementary function and integrated wiring of the evolutionarily distinct Drosophila olfactory subsystems. J. Neurosci. *31*, 13357–13375.

Stensmyr, M.C., Giordano, E., Balloi, A., Angioy, A.M., and Hansson, B.S. (2003). Novel natural ligands for Drosophila olfactory receptor neurones. J. Exp. Biol. *206*, 715–724.

Stökl, J., Strutz, A., Dafni, A., Svatos, A., Doubsky, J., Knaden, M., Sachse, S., Hansson, B.S., and Stensmyr, M.C. (2010). A deceptive pollination system targeting drosophilids through olfactory mimicry of yeast. Curr. Biol. *20*, 1846–1852.

Strutz, A., Völler, T., Riemensperger, T., Fiala, A., and Sachse, S. (2012). Calcium imaging of neural activity in the olfactory system of Drosophila. In Genetically Encoded Functional Indicators, Springer Protocols, J.R. Martin, ed. (New York: Springer), in press.

Vosshall, L.B., Wong, A.M., and Axel, R. (2000). An olfactory sensory map in the fly brain. Cell *102*, 147–159.

Wang, J.W., Wong, A.M., Flores, J., Vosshall, L.B., and Axel, R. (2003). Two-photon calcium imaging reveals an odor-evoked map of activity in the fly brain. Cell *112*, 271–282.

Wilson, R.I. (2008). Neural and behavioral mechanisms of olfactory perception. Curr. Opin. Neurobiol. *18*, 408–412.

Wilson, R.I., Turner, G.C., and Laurent, G. (2004). Transformation of olfactory representations in the Drosophila antennal lobe. Science *303*, 366–370.